Soft Dynamics simulation: 2. Elastic spheres undergoing a T1 process in a viscous fluid

Pierre Rognon, Cyprien Gay

Soft Dynamics simulation: 2. Elastic spheres undergoing a T1 process in a viscous fluid

Pierre Rognon and Cyprien Gay*
Centre de Recherche Paul Pascal, CNRS UPR 8641 - Av. Dr. Schweitzer, Pessac, France
Matière et Systèmes Complexes, Université Paris-Diderot - Paris 7, CNRS UMR 7057 - Paris, France
(Dated: January 1, 2009)

Robust empirical constitutive laws for granular materials in air or in a viscous fluid have been expressed in terms of timescales based on the dynamics of a single particle. However, some behaviours such as viscosity bifurcation or shear localization, observed also in foams, emulsions, and block copolymer cubic phases, seem to involve other micro-timescales which may be related to the dynamics of local particle reorganizations. In the present work, we consider a T1 process as an example of a rearrangement. Using the *Soft dynamics* simulation method introduced in the first paper of this series, we describe theoretically and numerically the motion of four elastic spheres in a viscous fluid. Hydrodynamic interactions are described at the level of lubrication (Poiseuille squeezing and Couette shear flow) and the elastic deflection of the particle surface is modeled as Hertzian. As expected from simple scaling predictions, we observe that the duration of the simulated T_1 process can be varied substantially by adjusting the elastic modulus of the particles and their initial separations. This provides hints for simple rheological models of granular materials.

PACS numbers: 02.70.Ns, 82.70.-y, 83.80.Iz

I. INTRODUCTION

Foams, emulsions and granular materials are made of interacting particles, respectively bubbles, droplets and grains, in a surrounding fluid. A great deal of research revealed their elastic, plastic and viscous characters [1, 2]. Some insight into their rheological behaviour was obtained by considering the dynamics of a single particle. Thus emerged the time $\sqrt{m/RP}$ for a single grain of mass m, accelerated by the normal stress P (force PR^2), to move over a distance comparable to its own size R [3, 4, 5], the time η/P for a grain immersed in a fluid of viscosity η subjected to the same normal stress [6], and the relaxation time $\eta R^2/\sigma$ for a bubble or a droplet with surface tension σ in a viscous fluid [7, 8, 9]. The effective viscosity was expressed as an empirical function of these microscopic timescales [6], thereby providing robust scaling expressions for various properties of grains [10, 11, 12] and bubbles [13, 14, 15, 16, 17, 18]. More recently, a two-particle argument [19], based on the same physics, provided a full prediction for the effective viscosity of dry or immersed grains, with an expression quite similar to the empirical function [6], and which justifies its frictional form.

Nevertheless, particulate materials exhibit some additional and uncommon rheological properties which seem to involve other timescales. For instance, a delayed adaptation of the shear rate to a sudden change in the applied stress [20, 21, 22, 23, 24, 25], and a critical shear rate below which no homogeneous flow exists have been observed [3, 4, 6, 21, 26]. Both are qualitatively understood as arising from the competition between external solicitations which disturb the particle network and some spontaneous reorganization process [21]. Getting new insights into reorganization micro-timescale should therefore clarify the origin of such properties and could also provide hints to refine and generalize existing models of the material response. It may also be useful to predict the coexistence of liquid and solid regions (shear localization, shear banding, cracks) as observed with emulsions [27, 28], foams [29, 30, 31, 32], wormlike micelles [33, 34] and granular materials [4, 12, 35, 36].

The common feature of many of these physical systems is that they are made of rather soft particles immersed in a viscous fluid. When such a complex fluid is subjected to deformation, especially in a rather dense configuration, the flow between neighbouring particles interplays with the particle deformability in a non-trivial manner. As this feature was ignored so far in existing simulations such as Molecular Dynamics [37] (for elastic grains without a surrounding fluid) or Stokesian Dynamics [38] (for non-deformable grains in a viscous fluid), we are introducing a new discrete numerical method, named *Soft Dynamics*, in a series of papers. In a first paper [39], we illustrated this interplay by simulating the normal interactions between two elastic particles in a viscous fluid. We showed that such a system indeed exhibits two distinct dynamics, for the center-to-center and surface-to-surface distances.

In this paper, again with purely elastic spheres in a Newtonian fluid, we investigate the dynamics of four interacting objects with both normal and tangential relative motion [55]. This will serve as an introduction to the principle of larger scale simulations with this new method, which should constitute a promising tool for investigating the collective behaviors of many complex materials.

More precisely, we focus on the dynamics of a T_1 process. This is a rather common reorganization process, depicted schematically on Fig. 1: two particles separate while two other particles establish contact. Meanwhile, the other particle pairs reorient, as shown by the evolution of angle θ from about $\frac{\pi}{3}$ to about $\frac{\pi}{6}$. Such T_1 processes occur in deformed regions of foams and emulsions, at a frequency proportional to the deformation rate (see for exam-

*Electronic address: cyprien.gay@univ-paris-diderot.fr

ple [29, 30, 40, 41, 42, 43, 44, 45, 46, 47]). As local plastic deformation events, they relax some stress while dissipating some energy. The duration of a T_1 is thus expected to affect the rheological behaviour of the material. For dry foams, the T_1 dynamics has been shown to result from the surface tension and the surface viscosity [48], with a negligible contribution from the viscosity of the surrounding fluid squeezed between the approaching bubbles. By contrast, such processes are less well described in wet foams or other less concentrated systems: visco-elastic and even adhesive properties were shown to be important [49, 50, 51], and we expect the squeezing of the surrounding liquid to play a significant role too.

In the following, we first present the interactions between the elastic particles (Section II). We then provide the main steps of the implementation of the *Soft Dynamics* method in the present context (Section III). Next, we derive theoretically the expected behaviour, in particular we discuss under which circumstances a T_1 process should indeed occur and (if it does occur) how long are the successive stages of the corresponding evolution (Section IV A). We finally present and discuss the numerical results (Section IV B).

II. MODELLING PARTICLE INTERACTIONS

When adressing the question of a T_1 process between elastic spheres in a viscous fluid, see Fig. 1, most of the interactions have already been described in the first paper [39]. The only new feature is particle sliding and, correspondingly, tangential forces. Hence, quantities such as viscous friction coefficients or spring constants are now tensorial.

A. Pairwise interactions

As discussed in detail in the first paper [39], because we consider rather dense systems where each particle is close to several other particles (surface-to-surface gap much smaller than the particle size), we simply discard long-range, many-body interactions (see for instance Ref. [52] for a presentation of such interactions). Furthermore, under such thin gap conditions, the interacting region between particles is much smaller than the particle size and the interactions between a particle and its neighbours are mostly independent from each other and can therefore be treated as a sum of pairwise interactions.

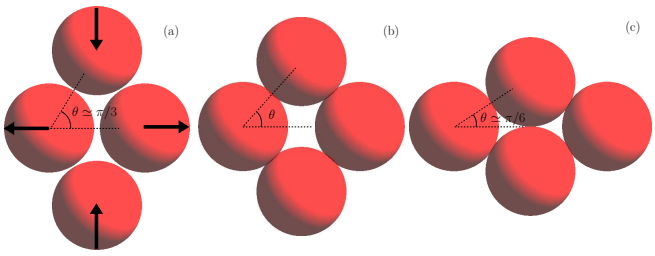

FIG. 1: Schematic representation of a T_1 process. Due to the applied forces, the group of four particles swap neighbours. The process is monitored through angle θ.

Due to the neighbouring particle j, the surface of particle i is deflected elastically as a result of *(i)* the local pressure field in the fluid that results from a viscous lubrication interaction and *(ii)* a remote interaction (such as a damped electrostatic interaction, steric repulsion, van der Waals interactions, disjoining pressure, etc):

$$\vec{F}_{ij}^{ela} = \vec{F}_{ij}^{vis} + \vec{F}_{ij}^{rem} \tag{1}$$

Besides, because the particle inertia can be neglected due to the dominant effect of the fluid viscosity, the sum of all forces applied to particle i vanishes:

$$\vec{F}_i^{ext} + \sum_j \vec{F}_{ij}^{ela} = 0 \tag{2}$$

where $\vec{F}_i^{ext}$ is an external force acting on grain i (such as gravity) and where the sum runs over the neighbours of particle i.

In principle, there is another equation, similar to Eq. (2), for the torques applied to particle i. But as mentioned earlier [55], this is not needed for the present symmetric T_1 configuration such as that of Fig. 1.

The *Soft Dynamics* method [39] simulates the dynamics of such a system, determined by the system of Eqs (2) for all particles i. In the present work, for simplicity, we omit the remote interactions in Eq. (1) as we did before [39].

In order to specify the elastic and viscous forces, let us now describe the geometry and the kinematics of the interacting region between a pair of neighbouring particles.

B. Contact geometry and kinematics

Let i and j denote two interacting particles, as depicted on Fig. 2. As compared to the first paper, the positions of the particles centers are now vectors, labeled $\overrightarrow{OX_i}$ and $\overrightarrow{OX_j}$, and $\vec{X}_{ij} = \overrightarrow{OX_j} - \overrightarrow{OX_i}$ is the center-to-center vector. The deflections of the particle surfaces are also vectors, labeled $\vec{\delta}_i^j$ and $\vec{\delta}_j^i$. Since all particles are identical and since the (lubrication) forces are pairwise and act locally, facing deflections are symmetric: $\vec{\delta}_i^j + \vec{\delta}_j^i = 0$. Thus, for simplicity, we shall use the total deflection $\vec{\delta}_{ij} = \vec{\delta}_i^j - \vec{\delta}_j^i$ for each pair of interacting particles. The unit vector normal to the contact can be expressed as

$$\vec{n}_{ij} = \frac{\vec{X}_{ij} - \vec{\delta}_{ij}}{|\vec{X}_{ij} - \vec{\delta}_{ij}|} \tag{3}$$

The gap h_{ij} between both particle surfaces depends on both the center-to-center vector $\vec{X}_{ij}$ and the total deflection $\vec{\delta}_{ij}$:

$$h_{ij} = |(\vec{X}_{ij} - \vec{\delta}_{ij}| - 2R, \tag{4}$$

Similarly, the relative velocity of the material points that constitute each particle surface, $\vec{v}_s$, involves the translation velocity of the particles (as already mentioned [55], the particles

do not rotate in the present situation) and the evolution of the surface deflection:

$$\vec{v}_s = \dot{\vec{X}}_{ij} - \dot{\vec{\delta}}_{ij}. \tag{5}$$

In order to specify viscous and elastic interactions, we will need to deal with projectors and tensors. We will use the symbol "$\cdot$" for the tensor product (contraction of one coordinate index), and $\vec{u}^T$ will denote the transposed of vector $\vec{u}$. Hence, $\vec{u}^T \cdot \vec{v} = \vec{v}^T \cdot \vec{u}$ will be the scalar product of $\vec{u}$ and $\vec{v}$, and $\vec{u} \cdot \vec{v}^T$ their outer product, which is a tensor. In particular, we will make use of tensor $\boldsymbol{\alpha}$ defined as the projector onto the normal direction:

$$\boldsymbol{\alpha} = \vec{n} \cdot \vec{n}^T \tag{6}$$

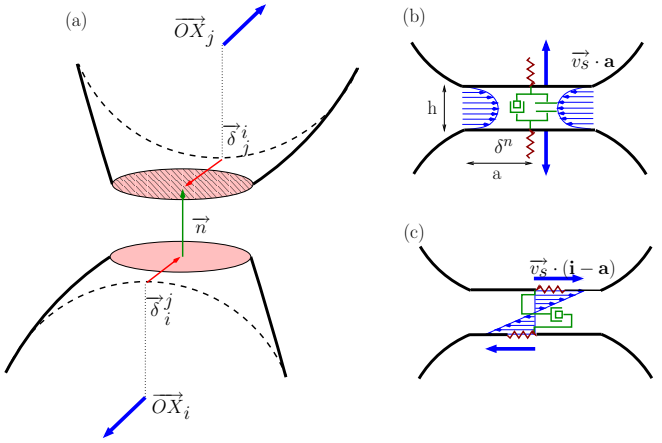

FIG. 2: Model of interaction for two elastic particles in a viscous fluid. (a) elastic deflection of the surfaces (in traction); (b) normal dissipation due to Poiseuille flow in the gap; (c) tangential dissipation due to the Couette flow. The force is transmitted from a particle to another through the fluid and through a possible remote force. Such a system behaves like a Maxwell fluid (a dashpot and a spring in series). The effective friction is a function of the gap h and of the size a of the surface through which the force is transmitted.

C. Viscous force

For a pair of close spheres, as discussed earlier [39], the fluid region that mediates most of the force between both particles has a large aspect ratio, and the flow is essentially parallel to the solid surfaces: the *lubrication approximation* can be used (see for example [53]). As before, the fluid inertia is negligible (low Reynolds numbers) and the viscous force $\vec{F}^{vis}$ acting on the surfaces depends linearly on their relative velocity $\vec{v}_s$:

$$\vec{F}^{vis} = \boldsymbol{Z} \cdot \vec{v}_s \tag{7}$$

$$\boldsymbol{Z} = \zeta\boldsymbol{\alpha} + \lambda(\mathbf{1} - \boldsymbol{\alpha}) \tag{8}$$

$$\zeta = \frac{3\pi\eta a^4}{2h^3} \tag{9}$$

$$\lambda = \frac{\pi\eta a^2}{h} \tag{10}$$

where the interparticle friction tensor $\boldsymbol{Z}$ has two components (normal and in-plane), expressed in terms of the unity tensor $\mathbf{1}$ and the projector $\boldsymbol{\alpha}$ defined by Eq. (6). The normal viscous friction ζ is related to the Poiseuille flow induced by squeezing or pulling [39] (see Fig. 2b), while the in-plane friction coefficient λ reflects the tangential motion (sliding) between both particles, which generates a Couette (shear) flow in the gap (see Fig. 2c).

D. Elastic force

Let us assume that the size a (discussed in the next paragraph) of the interacting region between particles i and j is known. Then, as before [39], the force depends linearly on the surface deflection, but this time the relation is tensorial:

$$\vec{F}^{ela} = a\boldsymbol{E} \cdot \vec{\delta}, \tag{11}$$

$$\boldsymbol{E} = E\left(c^n\boldsymbol{\alpha} + c^t(\mathbf{1} - \boldsymbol{\alpha})\right), \tag{12}$$

where the tensorial proportionality constant $\boldsymbol{E}$ is essentially the (scalar) Young modulus E, but incorporates geometrical constants on the order of unity c^n and c^t for the normal and tangential responses, respectively.

E. Size of the interacting region

The size of the interacting region, again [39], depends either on the gap thickness h (Poiseuille regime) when the particle surface is weakly deflected, or on the normal force (Hertz regime) when the particle surface can be considered planar.

In the first case, it can be expressed as $a \approx \sqrt{2Rh}$. In the second case, it is essentially independent of the tangential force [54] and can thus be expressed in terms of the normal deflection: $a \approx \sqrt{R|\delta^n|} = \sqrt{R|\vec{n}^T \cdot \vec{\delta}|}$. As explained earlier [39], for the purpose of the *Soft Dynamics* method, we interpolate between both behaviours of a in a simple manner:

$$a(h, \delta^n) = \sqrt{R(2h + |\delta^n|)}. \tag{13}$$

III. METHOD OF THE SOFT-DYNAMICS SIMULATION

The Soft-Dynamics method aims at simulating the time evolution of a system of elastic particles and in a viscous fluid, such as depicted in previous sections. Like usual discrete simulation methods, the motion of each particle center

results from the force balance, Eq. (2). The specificity is that the interaction evolution results from the decomposition of the center-to-center distance given by Eq. (4). As illustrated previously [39], this generates a Maxwellian contact dynamics through the combination of the elastic surface deflection and the viscous response of the fluid in the gap: it is possible to move the center-to-center distance $\overrightarrow{X}_{ij}$ while keeping constant the deflection $\overrightarrow{\delta}_{ij}$, and *vice-versa*. But as compared to a classical Maxwell behaviour, the elastic element does always behave linearly (Hertzian contact in the strong deflection regime), and the viscous element does not have a constant value, as it depend on the geometry of the gap, see Eqs. (7-10).

The Soft-Dynamics method consists in calculating the rate of change of all center positions $\overrightarrow{OX_i}$ and all gap deflections $\overrightarrow{\delta}_{ij}$ as a function of their current values, and integrating them over a small time step.

A. Equations of motion

The system satisfies one equation per interparticle interaction, namely Eq. (1), and one equation per particle, namely Eq. (2). We shall now see how it is possible to derive equations of motion. For this, we need to express the unknowns velocities $\dot{\overrightarrow{\delta}}_{ij}$ and $\dot{\overrightarrow{X}}_{ij}$ in terms of the current state of the system.

From Eqs. (3), (4) and (13), it appears that the size a of the interacting region can be expressed as a function of $\overrightarrow{X_{ij}}$ and $\overrightarrow{\delta}_{ij}$. It then follows from Eqs. (3) and (11) that the elastic force $\overrightarrow{F}^{ela}$ can also be expressed as a function of $\overrightarrow{X_{ij}}$ and $\overrightarrow{\delta}_{ij}$:

$$\overrightarrow{F}^{ela} = \overrightarrow{F}^{ela}(\overrightarrow{X_{ij}},\ \overrightarrow{\delta}_{ij}) \tag{14}$$

As a result, its time-derivative $\dot{\overrightarrow{F}}^{ela}_{ij}$ can be expressed as a sum two terms: one of them is linear in $\dot{\overrightarrow{X}}_{ij}$ while the other is linear in $\dot{\overrightarrow{\delta}}_{ij}$. The (tensorial) coefficient of each of these two terms is a function of the current system configuration, *i.e.*, of all particle and gap variables $\overrightarrow{OX_i}$ and $\overrightarrow{\delta}_{ij}$. Now, it follows from Eqs. (5), (7) and (1) that $\dot{\overrightarrow{\delta}}_{ij}$ is an affine function of $\dot{\overrightarrow{X}}_{ij}$:

$$\dot{\overrightarrow{\delta}}_{ij} = \dot{\overrightarrow{X}}_{ij} + \boldsymbol{Z}_{ij}^{-1} \cdot \left(\overrightarrow{F}^{ela}_{ij} - \overrightarrow{F}^{rem}_{ij} \right) \tag{15}$$

where $\boldsymbol{Z}_{ij}$, $\overrightarrow{F}^{ela}_{ij}$ and $\overrightarrow{F}^{rem}_{ij}$ depend on the current system configuration. Hence, $\dot{\overrightarrow{F}}^{ela}_{ij}$ can be expressed as an affine function of $\dot{\overrightarrow{X}}_{ij}$:

$$\dot{\overrightarrow{F}}^{ela}_{ij} = \boldsymbol{G}_{ij} \cdot \dot{\overrightarrow{X}}_{ij} - \overrightarrow{b}_{ij} \tag{16}$$

where the coefficients $\boldsymbol{G}_{ij}$ and $\overrightarrow{b}_{ij}$ depend only on the current system configuration. The detailed calculation of these coefficients is provided in Appendix A.

From this, the time derivative of Eq. (2) yields a system of equations for the particle center velocities. The equation that corresponds to particle i reads:

$$\sum_j \left\{ \boldsymbol{G}_{ij} \cdot (\dot{\overrightarrow{OX}}_j - \dot{\overrightarrow{OX}}_i) \right\} = \sum_j \overrightarrow{b}_{ij} - \dot{\overrightarrow{F}}^{ext}_i. \tag{17}$$

where the sums run over all neighbours of particle i.

Note that because $\boldsymbol{G}_{ji} = -\boldsymbol{G}_{ij}$ and $\overrightarrow{b}_{ji} = -\overrightarrow{b}_{ij}$, and if we assume that the sum of all external forces vanishes,

$$\sum_i \overrightarrow{F}^{ext}_i = 0, \tag{18}$$

then the sum of Eqs. (17) for all particles i vanishes. In other words, these vector equations are not independent: one of them must be replaced, for instance, by the condition that the average particle velocity is zero:

$$\sum_i \dot{\overrightarrow{OX}}_i = 0 \tag{19}$$

Let us consider the system of Eq. (19) (or a similar one) together with Eqs. (17), taken for all particles i except one. This system of equations can be inverted to obtain the particle center velocities $\dot{\overrightarrow{OX}}_i$. The gap velocities $\dot{\overrightarrow{F}}^{ela}_{ij}$ are then calculated from Eq. (16).

B. Choice of a numerical step

Gaining the center velocity $\dot{\overrightarrow{OX_i}}$ requires to solve the linear system (17). Standard and efficient procedures are available to inverse it. We used a second order Newtonian scheme for the numerical integration of particle position and as well as deflections. A typical time in the problem is the Stokes time τ taken by a single particle submitted to a typical force F to move over a distance R in a fluid with viscosity η, see Eq. (28) below. The numerical time step is set to 10^{-3} in units of τ for all simulations. Other numerical schemes, such as Runge Kutta method, should make simulations faster. Furthermore, a study of the optimal required time step will be necessary when dealing with significantly more than only four particles.

IV. T_1 DYNAMICS

Let us now use the Soft-Dynamics method to simulate a single T_1 process. The system is depicted on Fig. 3: initially, particles B and C are aligned horizontally, with a small gap h_0, while particles A and D are aligned vertically. The diagonal gaps (between A and B, etc) have thickness h_0 too.

A horizontal force N_x is applied on particles B and C while a vertical force N_y is applied on A and D. Various evolutions are possible depending on these two forces, which may or may not give rise to a T_1 process (see Fig. 3). Basically, a T_1 occurs only if the interaction between particles B and C is tensile. The criterion for the occurence of a T_1 process will be derived below, as well as a scaling for its dynamics. The duration of a T_1 will then be measured from the simulation.

A. Theoretical predictions

The T_1 process, which consists in a separation of the horizontal pair of particles (BC) and an approach of the vertical pair of particles (AD), implies some sliding of the diagonal pairs (see Fig. 1).

At the early stages of the process, when $\theta \approx \pi/3$, the external forces N_x and N_y can be expressed in terms of the normal forces in the horizontal (N_h) and diagonal (N_d) pairs of particles, and in terms of the sliding force S_d in the diagonal pairs:

$$N_x = N_h + 2\frac{1}{2}N_d - 2\frac{\sqrt{3}}{2}S_d \tag{20}$$

$$N_y = 2\frac{\sqrt{3}}{2}N_d + 2\frac{1}{2}S_d \tag{21}$$

In fact, as we shall now see, the tangential force S_d is much smaller than the normal forces. To show this, let us first notice that the tangential velocity is related to the angle θ defined on Fig. 1: $v_t \simeq -R\dot{\theta}$. In the Poiseuille regime, the particles

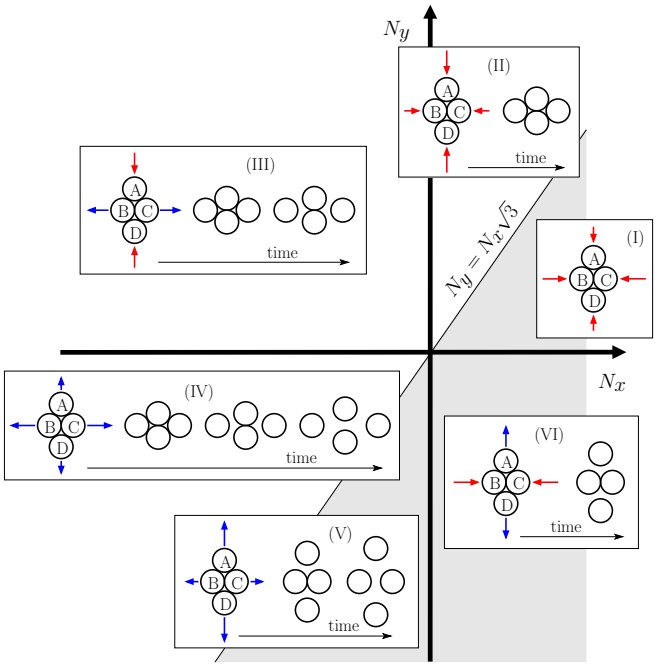

FIG. 3: Schematic evolution of four particles subjected to external forces. Force N_x is horizontal and acts on particles B and D. Force N_y is vertical and acts upon particles A and C. Both N_x and N_y can be either compressive (> 0) or tensile (< 0). Regimes (I) and (II) correspond to compressive forces. In regime (I), the configuration remains mostly unaltered. By contrast, a topological rearrangement (T_1 process) occurs when $N_y \gtrsim \sqrt{3}N_x$, which corresponds to region (II). When N_x or N_y is tensile, the four beads do not remain together, as can be seen from the time evolutions sketched for regimes (III)-(VI). On the whole, a T_1 process always occurs when $N_y \gtrsim \sqrt{3}N_x$ (regimes II, III and IV, white region). It is followed by particle separation when N_x is tensile (regimes III and IV). By contrast, no T_1 process occurs when $N_y \lesssim \sqrt{3}N_x$ (regimes I, V and VI, light grey region).

surfaces are weakly deflected and the horizontal and diagonal gaps are related to angle θ through $R + \frac{1}{2}h_h = (2R + h_d)\cos\theta$. Hence, the gap variations obey $\frac{1}{2}\dot{h}_h \approx \dot{h}_d\cos\theta - 2R\dot{\theta}\sin\theta$, *i.e.*:

$$\frac{1}{2}\dot{h}_h \approx \dot{h}_d\cos\theta + 2v_t\sin\theta \tag{22}$$

Let us now transform each term of the above equation by expressing it as a function of the corresponding normal or tangential force by using the appropriate friction coefficient as defined by Eq. (8):

$$-\frac{1}{2}\frac{N_h}{\zeta} \approx -\frac{N_d}{\zeta}\frac{1}{2} + 2\frac{S_d}{\lambda}\frac{\sqrt{3}}{2} \tag{23}$$

The relative magnitude of friction coefficients ζ and λ can be derived from Eqs. (9) and (10):

$$\frac{\zeta}{\lambda} = \frac{3}{2}\left(\frac{a}{h}\right)^2. \tag{24}$$

where the size a of the interaction region is given by Eq. (13). We thus have $\zeta/\lambda \approx R/h$ in the Poiseuille regime and $\zeta/\lambda \approx R\delta^n/h^2$ in the Hertz regime. Hence, except for very large gaps h comparable to the particle size R, the normal friction is much larger than the sliding friction: $\zeta \gg \lambda$. It follows that

$$S_d \simeq \frac{1}{2\sqrt{3}}\frac{\lambda}{\zeta}(N_d - N_h) \tag{25}$$

can be neglected in Eqs. (20–21). Hence, the interaction force within the horizontal pair BC depends only on the applied forces:

$$N_h \approx N_x - \frac{1}{\sqrt{3}}N_y \tag{26}$$

This implies that, as pictured on Fig. 3, the gap will open and the T_1 will proceed whenever N_h is tensile, *i.e.*, when $N_y \gtrsim N_x\sqrt{3}$ (white region of the diagramme). By contrast, the particles will not swap neighbours when $N_y \lesssim N_x\sqrt{3}$ (light grey region).

When N_h is indeed tensile, we now wish to determine how long it takes for the horizontal pair of particles to separate.

The dynamics of such a normal motion was detailed in Ref. [39]. Let us define the reduced force

$$\kappa = \frac{|N_h|}{ER^2} \tag{27}$$

and the Stokes time

$$\tau = \frac{6\pi\eta R^2}{|N_h|} \tag{28}$$

With the force N_h acting within the horizontal pair BC, the initial configuration (gap h_0) corresponds to the Poiseuille regime if $h_0 \gtrsim h_{HP}$ and to the Hertz regime if $h_0 \lesssim h_{HP}$, where

$$h_{HP} = R\,\kappa^{2/3} \tag{29}$$

The corresponding rate of change of the gap [39] can be expressed as:

$$\dot{h} = \frac{h}{\tau} \qquad \text{(Poiseuille, } h > h_{HP}) \tag{30}$$

$$\dot{h} = \frac{h^3}{\tau R^2}\kappa^{-\frac{4}{3}} \qquad \text{(Hertz, } h < h_{HP}). \tag{31}$$

Integrating these equations yields the typical time Δ required to achieve the separation of the horizontal pair BC of particles from an initial gap h_0 to a much larger gap $h_f \approx R$:

$$\Delta \simeq \tau \ln\left(\frac{h_f}{h_0}\right) \approx \tau \qquad \text{(Poiseuille, } h_0 > h_{HP}) \tag{32}$$

$$\Delta \simeq \tau\kappa^{\frac{4}{3}}\left(\frac{R^2}{h_0^2} - \frac{R^2}{h_{HP}^2}\right) + \tau\ln\left(\frac{h_f}{h_{HP}}\right) \approx \tau\kappa^{\frac{4}{3}}\frac{R^2}{h_0^2} \gg \tau \qquad \text{(Hertz, } h_0 < h_{HP}) \tag{33}$$

Once the gap h_h of the horizontal pair BC becomes comparable to R, the diagonal pairs such as AB slide rather quickly (since their $\lambda \ll \zeta$), and soon the gap h_v of the vertical pair AD becomes significantly smaller than R. The time it then takes to reach the same value h_0 is again comparable to Δ.

Hence, the order of magnitude given by Eqs. (32–33) for the time Δ is typically the expected order of magnitude for the duration of the entire T_1 process. We will now test this prediction by comparing it with the simulation results.

B. Result from simulations

We implement the *Soft Dynamics* method to simulate a T_1 process such as that depicted on Fig. 3, varying the two control parameters we pointed out above: the initial gap $10^{-3} < h_0/R < 0.8$ and the reduced force $10^{-4} < \kappa < 0.1$. For simplicity, there is no horizontal force ($N_x = 0$). The reduced force given by Eq. (27) is then equal to $\kappa = |N_y|/ER^2\sqrt{3}$ and the Stokes time is $\tau = 6\pi\sqrt{3}\eta R^2/|N_y|$.

Figure 4 displays the variations of several quantities in the course of a T_1 process with a given set of parameters ($h_0 = 10^{-2}R$, $\kappa = 3.10^{-3}$). In order to avoid discontinuities in the simulation, the force N_y is increased from zero to its nominal value within a time τ, and remains constant thereafter. From a macroscopic point of vue, for instance through the variation of the angle θ, the system seems to be almost blocked ($\theta \approx \pi/3$) for a significant amount of time ($t \lesssim 100\tau$). It then starts moving to reach its final configuration ($\theta \approx \pi/6$) where it remains thereafter ($t \gtrsim 250\tau$). During the "blocked" phase, the applied force N_y is transmitted through the diagonal interaction such as AB, thereby inducing a tensile force $N_h \approx -N_y/\sqrt{3}$ in the horizontal pair BC. Hence, despite the overal "blocked" appearence of the system, the horizontal gap h_h between particles B and C slowly increases from its initial value h_0. Correspondingly, the horizontal friction deacreases.

The fast moving period starts as soon as this friction is low enough. Particles B and C then separate quickly while particles A and D in the vertical pair approach each other, thereby giving rise to sliding friction on the diagonal interactions. As particles A and D approach, the corresponding gap h_v deacreases and the friction increases. This approach then slows down. Thus, although the system keeps moving, it *appears* to reach a new "blocked" configuration, with no more sliding or horizontal traction, but only a vertical compression.

As the system subjected to a constant force keeps moving, we need to arbitrarily define the end of the T_1 process. Among various possible choices, we shall here consider that the T_1 process is completed when the vertical interaction transmits most of the applied force ($N_v = 0.99\,N_y$). The resulting duration of the T_1 process is plotted on Fig. 5 (other criteria would yield similar results). The first observation is that, for the range of inital gaps and particle stiffnesses we consider, the duration of the T_1 is distributed over a wide range of timescales, roughly between 3τ and $10^3\tau$. Next, we observe that these results match our theoretical predictions reasonably:

- if the horizontal pair BC is in the Poiseuille regime, the T_1 duration Δ scales like $\tau\ln(R/h_0)$. It thus depends on particle radius, on the applied force and on the fluid viscosity through τ, as can be seen from Eq. (28), and sligthly on the inital gap through the logarithmic factor. The T_1 duration is then just a few times larger than the Stokes time τ;
- if pair BC is in the Hertz regime, the T_1 duration Δ scales essentially like $\tau\kappa^{\frac{4}{3}}\left(\frac{R}{h_0}\right)^2$, which implies a much stronger dependance on h_0, and longer durations since the particles are soft. In this case, Δ can be much longer than the Stokes time τ.

Note that in the latter case, the separating pair of particles leave the Hertz regime and enter the Poiseuille regime in the late stages of separation ($h > h_{HP}$). However, because the evolution is much slower in the Hertz regime, see Eqs. (30–31), these late Poiseuille stages contribute very weakly to the overall T_1 duration Δ.

In summary, the numerical result for the duration of a T_1 process presented on Fig. 5 are compatible with Eqs. (32–33). They demonstrate that the duration of a T_1 is hardly larger than the Stokes time τ given by Eq. (28) as long as the surface deflection is small compared to the inter-particle gap (Poiseuille regime) and thus depend mainly on the applied force, on the fluid viscosity and on the particle size. Remarkably, in the opposite regime where the deflection is larger than the gap (Hertz regime), the T_1 duration depends strongly on the interparticle gap and can reach very large values, as illustrated by Fig. 5.

V. CONCLUSION

Elastic particles interacting closely in a viscous fluid may exhibit various microscopic timescales during their relative motions. In the present paper, we focused on the dynamics of a T_1 process, as it is a common local plastic event in particulate materials. Its typical duration Δ studied in the present work should play an important role in the macroscopic behaviour

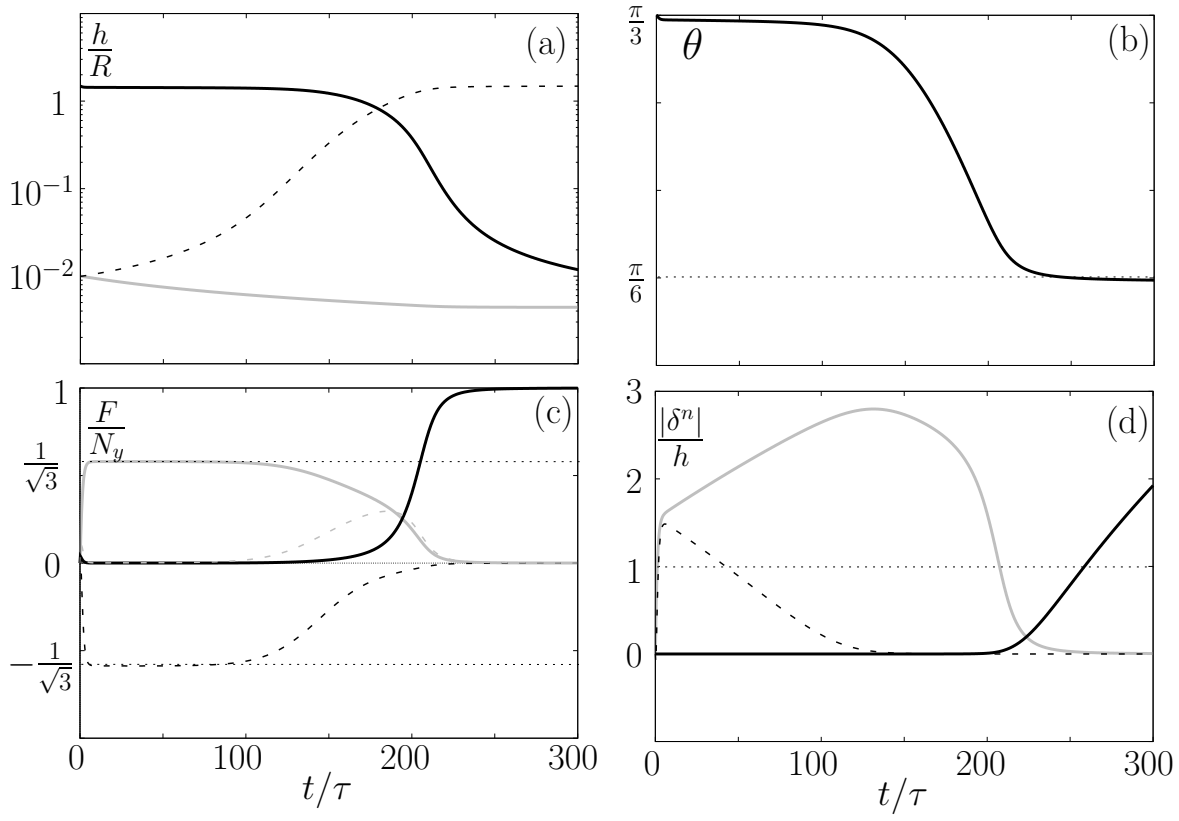

FIG. 4: Time evolution of various quantities in the course of a T_1 process, wth parameters $\kappa = 310^{-3}$, $h_0 = 10^{-2}R$ and $N_x = 0$. The gap h *(a)*, the normal and tangential forces *(c)* and the ratio $|\delta^n|/h$ *(d)* are plotted for the vertical (solid black lines, *AD*), the horizontal (dotted black lines, *BC*) and the diagonal (solid grey lines, *AB* etc) pairs of particles. On graph *(c)*, the dotted grey line represents the tangential force S_d of a diagonal pair such as *AB* (which is zero for the vertical pair *AD* and horizontal pair *BC*). Graph *(b)* shows the angle θ such as defined on Fig. 1. On graph *(d)*, a pair of particles for which $|\delta^n|/h > 1$ is in the Hertz regime. If $|\delta^n|/h < 1$, it is in the Poiseuille regime.

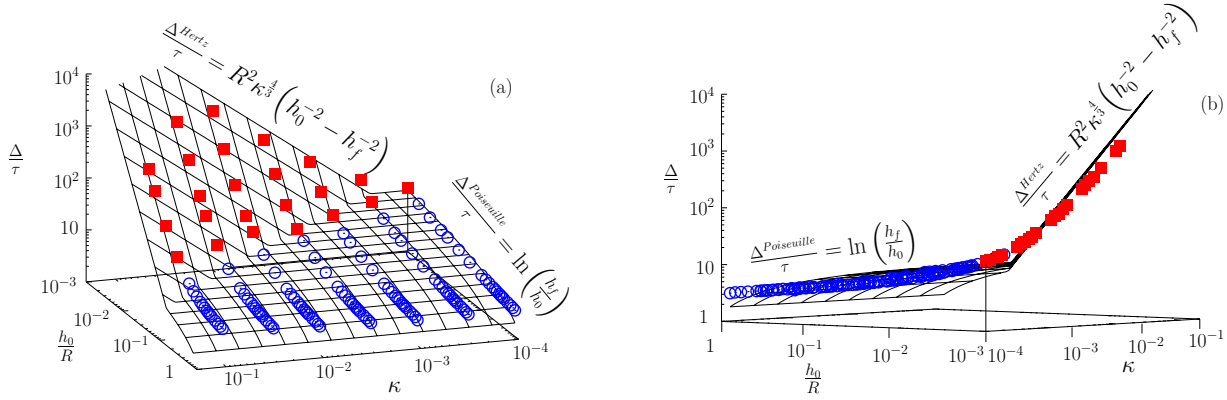

FIG. 5: (Color online) Typical duration Δ of a T_1 process as a function of the initial gap h_0 and of the adimensionalized applied force κ. The data points were obtained through the Soft-Dynamics simulation presented here. Blue open circles correspond to T_1s where the horizontal pair has remained in the Poiseuille regime during the entire process. Full red squares correspond to T_1s, such as that represented on Fig. 4, whose horizontal (separating) pair has been in the Hertz regime for part of the time. The surface is that defined by the theoretical model for both regimes (Eqs. 32–33 with $h_f = 2.5R$).

of the material, especially in some phenomena mentioned in the Introduction, such as a delayed adaptation of the shear rate

to a sudden change in the applied stress [20, 21, 22, 23, 24, 25] or the existence of a critical shear rate below which no homogeneous flow can survive [3, 4, 6, 21, 26].

More specfically, the present study, summarized by the results presented on Figs. 4 and 5, shows that for a given material (particle size and elastic modulus, fluid viscosity) the duration of a T_1 process is strongly dependent on the typical gap h_0 between neighbouring particles. Microscopic ingredients such as this one will need to be tested and refined in larger scale simulations. Meanwhile, combined with other ingredients, they may serve as a ground to outline more elaborate assumptions and refine existing simple rheological models for granular materials. In particular, the present study strongly suggests that in a granular material immersed in a viscous fluid, the typical gap h_0 between neighbouring particles or a similar parameter should constitute an essential ingredient to determine the plastic dynamics of the material, and should therefore be used instead of, or in combination with, the usual particle volume fraction criterion.

Acknowledgments

We gratefully acknowledge fruitful discussions with François Molino and with participants of the GDR 2983 Mousses (CNRS). This work was supported by the Centre National de la Recherche Scientifique (CNRS), by the Université Paris-7 Paris Diderot, and by the Agence Nationale de la Recherche (ANR-05-BLAN-0105-01).

APPENDIX A: DYNAMICS OF PARTICLES

In this Appendix, we deduce the particle dynamics, given by Eqs. (17), from the physical model of interactions and the mechanical equilibria described in Sec. III. We start from the time derivative of the particle force balance given by Eq. (2):

$$\sum_j \dot{\overrightarrow{F}}_{ij}^{ela} + \dot{\overrightarrow{F}}_i^{ext} = 0, \tag{A1}$$

Let us express the aboveas a sum of *(i)* $\dot{\overrightarrow{F}}_i^{ext}$ which is supposed to be known, *(ii)* terms that are linear in the particle center velocities, and *(iii)* another term that is explicitly known from the current state of the system, *i.e.*, from $\overrightarrow{X}_{ij}$ and $\overrightarrow{\delta}$. To this aim, using Eq. (11), let us express $\dot{\overrightarrow{F}}_{ij}^{ela}$ in terms of the partial derivative of $\overrightarrow{F}^{ela}(a, \boldsymbol{E}, \overrightarrow{\delta})$:

$$\dot{\overrightarrow{F}}_{ij}^{ela} = \frac{a}{2}\boldsymbol{E}\cdot\dot{\overrightarrow{\delta}} + \frac{a}{2}\dot{\boldsymbol{E}}\cdot\overrightarrow{\delta} + \dot{a}\frac{\boldsymbol{E}\cdot\overrightarrow{\delta}}{2}. \tag{A2}$$

1. Combination

We can now easily express each terms of Eq. (A2) as a function of $\dot{\overrightarrow{X}}_{ij}$. The first term is directly given by (5):

$$\frac{a}{2}\boldsymbol{E}\cdot\dot{\overrightarrow{\delta}} = \boldsymbol{G_1}\cdot\dot{\overrightarrow{X}}_{ij} - \overrightarrow{b}_1 \tag{A3}$$

$$\boldsymbol{G_1} = \frac{a}{2}\boldsymbol{E} \tag{A4}$$

$$\overrightarrow{b}_1 = \boldsymbol{G_1}\cdot\overrightarrow{v}_s \tag{A5}$$

The second term involves the time derivative $\dot{\boldsymbol{E}} = E(c_n - c_t)\dot{\boldsymbol{\alpha}}$ of the contact stiffness expressed by Eq. (12). Using (A13), it can be expressed as:

$$a\frac{\dot{\boldsymbol{E}}}{2}\cdot\overrightarrow{\delta} = -\overrightarrow{b}_2 \tag{A6}$$

$$\overrightarrow{b}_2 = -\frac{aE(c_n - c_t)}{2}\dot{\boldsymbol{\alpha}}\cdot\overrightarrow{\delta} \tag{A7}$$

Note that this term vanishes for $c_n = c_t$.

The third term involves the time derivative of a, which we express through its partial derivatives: $\dot{a}(\delta^n, h) = a_{\delta^n}\dot{\delta}^n + a_h\dot{h}$ (we used the notation $a_{\delta^n} = \frac{\partial a}{\partial \delta^n}$ and $a_h = \frac{\partial a}{\partial h}$). Replacing $\dot{\delta}^n$ and $\dot{h}$ by their respective expressions in terms of $\dot{\overrightarrow{X}}_{ij}$, Eqs. (A14) and (A15) lead to:

$$\dot{a}\frac{\boldsymbol{E}\cdot\overrightarrow{\delta}}{2} = \boldsymbol{G_3}\cdot\dot{\overrightarrow{X}}_{ij} - \overrightarrow{b}_3 \tag{A8}$$

$$\boldsymbol{G}_3 = \frac{a_{\delta^n}}{2}\boldsymbol{E}\cdot\overrightarrow{\delta}\cdot\overrightarrow{n}^T \tag{A9}$$

$$\overrightarrow{b}_3 = \frac{\boldsymbol{E}\cdot\overrightarrow{\delta}}{2}\left[a_{\delta^n}\left(\overrightarrow{v}_s{}^T\cdot\overrightarrow{n} - \overrightarrow{\delta}^T\cdot\dot{\overrightarrow{n}}\right) - a_h\dot{h}\right] \tag{A10}$$

Finally, substituting the three results of Eqs. (A3), (A6) and (A8) into Eq. (A2) yields:

$$\boldsymbol{G}\cdot\dot{\overrightarrow{X}}_{ij} = \overrightarrow{b} + \dot{\overrightarrow{F}}_{ij}^{ela} \tag{A11}$$

where $\boldsymbol{G} = \boldsymbol{G_1} + \boldsymbol{G_3}$ and $\overrightarrow{b} = \overrightarrow{b}_1 + \overrightarrow{b}_2 + \overrightarrow{b}_3$ are two explicit functions of $\overrightarrow{\delta}$ and $\overrightarrow{X}_{ij}$ Then, for each particle i, summing on its interacting particles j and using the force balance (2) yields the system of equation (17).

2. Preliminary differentiations

According to the definition of the normal vector, $\overrightarrow{n} = \frac{\overrightarrow{X_{ij}} - \overrightarrow{\delta}}{|\overrightarrow{X_{ij}} - \overrightarrow{\delta}|}$, and to that of the associated projector, $\boldsymbol{\alpha} = \overrightarrow{n}\cdot\overrightarrow{n}^T$, we obtain their time derivatives:

$$\dot{\overrightarrow{n}} = (\mathbf{1} - \boldsymbol{\alpha})\cdot\frac{\overrightarrow{v}_s}{|\overrightarrow{X_{ij}} - \overrightarrow{\delta}|} \tag{A12}$$

$$\dot{\boldsymbol{\alpha}} = \dot{\overrightarrow{n}}\cdot\overrightarrow{n}^T + \overrightarrow{n}\cdot\dot{\overrightarrow{n}}^T \tag{A13}$$

as two an explicit functions of $\overrightarrow{\delta}$ and $\overrightarrow{X}_{ij}$. Indeed, according to Eq. (15), $\overrightarrow{v}_s$ can be expressed as a function of the elastic force: $\overrightarrow{v}_s = \boldsymbol{Z}^{-1} \cdot \left(\overrightarrow{F}^{ela} - \overrightarrow{F}^{rem} \right)$.

The evolution of the normal deflection $\delta^n = \overrightarrow{\delta}^T \cdot \overrightarrow{n}$ can be expressed as a function of $\overrightarrow{X}_{ij}$ by using Eqs. (A12) and (5):

$$\begin{aligned} \dot{\delta^n} &= \dot{\overrightarrow{\delta}}^T \cdot \overrightarrow{n} + \overrightarrow{\delta}^T \cdot \dot{\overrightarrow{n}} \\ &= \dot{\overrightarrow{X}}_{ij}^T \cdot \overrightarrow{n} - \overrightarrow{v}_s{}^T \cdot \overrightarrow{n} + \overrightarrow{\delta}^T \cdot \dot{\overrightarrow{n}} \end{aligned} \qquad \text{(A14)}$$

Finally, from Eq. (5), we deduce the expression of the gap evolution $\dot{h}$ as a function of $\dot{\overrightarrow{X}}_{ij}$:

$$\dot{h} = \left(\overrightarrow{X_{ij}} - \overrightarrow{\delta} \right) \cdot \dot{\overrightarrow{n}} + \overrightarrow{v}_s \cdot \overrightarrow{n}. \qquad \text{(A15)}$$

[1] D. Weaire and S. Hutzler, *The Physics of Foams* (Oxford University Press, 2001).
[2] P. Coussot, *Rheometry of pastes, suspensions, and granular materials* (Wiley-Interscience, 2005).
[3] GDR MiDi, Euro. Phys. J. E **14**, 341 (2004).
[4] F. da Cruz, S. Emam, M. Prochnow, J.-N. Roux, and F. Chevoir, Phys. Rev. E **72**, 021309 (2005).
[5] Y. Forterre and O. Pouliquen, Annu. Rev. Fluid Mech. **40**, 1 (2008).
[6] C. Cassar, M. Nicolas, and O. Pouliquen, Phys. Fluids **17**, 103301 (2005).
[7] D. J. Durian, Phys. Rev. Lett. **75**, 4780 (1995).
[8] D. Durian, Phys. Rev. E **55**, 1739 (1997).
[9] P. Sollich, F. Lequeux, P. Hraud, and M. Cates, Phys. Rev. Lett. **78**, 102020 (1997).
[10] P. Jop, Y. Forterre, and O. Pouliquen, Nature **441**, 727 (2006).
[11] P. Rognon, J. Roux, M. Naaïm, and F. Chevoir, Phys. Fluids **19**, 058101 (2007).
[12] P. G. Rognon, J.-N. Roux, M. Naaim, and F. Chevoir, J. Fluid Mech. **596** (2008).
[13] S. Tewari, D. Schiemann, D. J. Durian, C. M. Knobler, S. A. Langer, and A. J. Liu, Phys. Rev. E **60**, 4385 (1999).
[14] A. Gopal and D. Durian, J. Coll. Inter. Sci. **213**, 169 (1999).
[15] B. Gardiner, B. Dlugogorski, and G. Jameson, J. Non Newtonian Fluid Mech. **92**, 151 (2000).
[16] B. Gardiner, B. Dlugogorski, and G. Jameson, J. Phys. : Cond. Mat. **11**, 5437 (1999).
[17] B. Gardiner and A. Tordesillas, J. Rheol. **49**, 819 (2005).
[18] M. Kern, F. Tiefenbacher, and J. McElwaine, Cold Regions Sciences and Technology **39**, 181 (2004).
[19] P. Rognon and C. Gay, submitted (2008), hal/arxiv.
[20] F. da Cruz, F. Chevoir, D. Bonn, and P. Coussot, Phys. Rev. E **66**, 051305 (2002).
[21] P. Coussot, Q. Nguyen, H. Huynh, and D. Bonn, J. Rheol. **43**, 1 (2002).
[22] F. Rouyer, S. Cohen-Addad, M. Vignes-Adler, and R. Höhler, Phys. Rev. E **67**, 021405 (2003).
[23] P. Coussot, H. Tabuteau, X. Chateau, L. Tocquer, and G. Ovarlez, J. Rheol. **50**, 975 (2006).
[24] E. Eiser, F. Molino, G. Porte, and X. Pithon, Rheologica Acta **39**, 201 (2000).
[25] E. Eiser, F. Molino, G. Porte, and O. Diat, Phys. Rev. E **61**, 6759 (2000).
[26] P. G. Rognon, F. Chevoir, H. Bellot, F. Ousset, M. Naaim, and P. Coussot, J. Rheol. **52** (2008).
[27] P. Coussot, J. Raynaud, P. Moucheront, J. Guilbaud, and H. Huynh, Phys. Rev. Lett. **88**, 218301 (2002).
[28] L. Bécu, S. Manneville, and A. Colin, Phys. Rev. Lett. **96**, 138302 (2006).
[29] G. Debrégeas, H. Tabuteau, and J. di Meglio, Phys. Rev. Lett. **87**, 178305 (2001).
[30] A. Kabla and G. Debrégeas, Phys. Rev. Lett. **90**, 258303 (2003).
[31] E. Janiaud, D. Weaire, and S. Hutzler, Phys. Rev. Lett. **97**, 38302 (2006).
[32] E. Janiaud, D. Weaire, and S. Hutzler, Colloids and Surfaces A: Physicochemical and Engineering Aspects **309**, 125 (2007).
[33] J. Salmon, A. Colin, S. Manneville, and F. Molino, Phys. Rev. Lett. **90**, 228303 (2003).
[34] L. Bécu, D. Anache, S. Manneville, and A. Colin, Physical Review E **76**, 11503 (2007).
[35] N. Huang, G. Ovarlez, F. Bertrand, S. Rodts, P. Coussot, and D. Bonn, Phys. Rev. Lett. **94**, 28301 (2005).
[36] P. Mills, P. Rognon, and F. Chevoir, Europhys. Lett. **81**, 64005 (2008).
[37] P. A. Cundall and O. D. L. Strack, Gotech. **29**, 47 (1979).
[38] L. Durlofsky, J. Brady, and G. Bossis, J. Fluid Mech. **180**, 21 (1987).
[39] P. Rognon and C. Gay, Eur. Phys. J. E **27**, 253 (2008).
[40] H. Princen, J. Coll. Inter. Sci. **91**, 160 (1983).
[41] T. Okuzono and K. Kawasaki, J. Rheol. **37**, 571 (1993).
[42] J. C. Earnshaw and A. H. Jaafar, Phys. Rev. E **49**, 5408 (1994).
[43] Y. Jiang, P. J. Swart, A. Saxena, M. Asipauskas, and J. Glazier, Phys. Rev. E **59**, 5819 (1999).
[44] S. Cohen-Addad and R. Höhler, Phys. Rev. Lett. **86**, 4700 (2001).
[45] A. D. Gopal and D. J. Durian, Phys. Rev. Lett. **91**, 188303 (2003).
[46] M. Dennin, Phys. Rev. E **70**, 41406 (2004).
[47] S. Vincent-Bonnieu, R. Höhler, and S. Cohen-Addad, Europhysics Letters **74**, 533 (2006).
[48] M. Durand and A. Stone, Phys. Rev. Lett. **97**, 226101 (2006).
[49] M.-D. Lacasse, G. S. Grest, and D. Levine, Phys. Rev. E **54**, 5436 (1996).
[50] S. Besson and G. Debrégeas, The European Physical Journal E-Soft Matter **24**, 109 (2007).
[51] M. Lacasse, G. Grest, D. Levine, T. Mason, and D. Weitz, Phys. Rev. Lett. **76**, 3448 (1996).
[52] G. Abade and F. Cunha, Computer Methods in Applied Mechanics Engineering **196**, 4597 (2007).
[53] G. K. Batchelor, *An introduction to fluid dynamics* (Cambridge University Press, Cambridge, 1967).
[54] K. L. Johnson, *Contact Mechanics* (Cambridge University Press, Cambridge, 1985).
[55] As the particle configuration we consider is symmetric, it is not necessary to include particle rotation at this stage: it will be introduced in a forthcoming paper.